Ac Conductivity and Dielectric Properties of Amorphous $Ge_{15}Se_{60}X_{25}$ (X = As or Sn) Films

N.A. Hegab, M.A. Afifi, H.E. Atyia and M.I. Ismael
Physics Department, Faculty of Education, Ain Shams University, Cairo, Egypt

(Received May 8, 2010; in final form October 11, 2010)

The ac conductivity and dielectric properties of $Ge_{15}Se_{60}X_{25}$ (X = As or Sn) thin films are reported in this paper. The thin films were deposited by thermal evaporation at 10^{-5} Torr pressure. The films were well characterized by X-ray diffraction, differential thermal analysis and energy dispersive X-ray spectroscopy. The ac conductivity was measured over temperature range 303–413 K and frequency range 10^2–10^5 Hz. The frequency dependence of the ac conductivity was found to be linear with slope which lies very close to unity and is independent of temperature. This behavior can be explained in terms of the correlated barrier hopping between centers forming intimate valence alternation pairs. Values of the dielectric constant ε_1 were found to decrease with frequency and increase with temperature. The maximum barrier height W_m for each sample, which was calculated from the dielectric measurements according to the Guinitin equation, agrees with the theory of hopping of charge carriers over potential barrier as suggested by Elliott in case of chalcogenide glasses. The density of localized state near the Fermi level was estimated for the studied films.

PACS: 72.80.Ng, 77.22.–d

1. Introduction

Chalcogenide glasses have received a great deal of attention for the last two decades due to their technological applications, namely electronic, optoelectronic, optical and memory switching devices, guided wave devices and infrared telecommunication systems [1–6].

Chalcogenides like Ge–Se are known to be very good covalent bonded glass formers. It has been established that the physical properties of this system are highly composition dependent [7–10]. It is found that the properties of this class of amorphous material are usually affected by the addition of impurities as a third element. Recently a lot of attention has been paid to achieve the influence of impurities on the physical properties of chalcogenides [11–13].

The ac conductivity and dielectric properties provide a fundamental method to understand the nature of conduction and defect centers present in the chalcogenide glass systems. Different models [14–18] have been proposed to interpret the mechanism of ac conduction.

The present paper reports the temperature and frequency dependent ac conductivity for film samples of $Ge_{15}Se_{60}X_{25}$ (X = As or Sn). The proper conduction mechanism can be characterized from this study. The frequency and temperature dependence of the dielectric constant ε_1 and dielectric loss ε_2 are studied. These studies are carried out in the frequency range 10^2–10^5 Hz and temperature range 303–413 K through the thickness range (89–903 nm).

2. Experimental details

$Ge_{15}Se_{60}As_{25}$ and $Ge_{15}Se_{60}Sn_{25}$ compositions were synthesized as follows: the elementary constituents of each composition of purity 99.999% were weighed in accordance with their atomic percentage and loaded in a silica tube, which was then sealed under vacuum (10^{-5} Torr). The content of each tube was heated gradually in an oscillatory furnace to 500 K (melting point (m.p.) of Se or Sn) and kept constant for 1 h and raised to 880 K (m.p. of As) and kept constant for 1 h and finally it was raised to 1273 K (> m.p. of Ge) and kept constant for 24 h. Long time of synthesis and oscillation of the tube are necessary for the homogeneity of the synthesized compositions. The tube is then quenched in icy water to obtain the compositions in the glassy state. Measurements of the density of the prepared bulk compositions were made by the Archimedes method [19]. The values of the density thereby obtained are used in the data of the program in thickness monitor connected to the coating unit to control the thickness of the films.

Thin films of the investigated compositions were obtained from bulk samples by thermal evaporation technique under vacuum and subsequent deposition on high cleaned glass substrates for electrical measurements.

The substrates were fixed onto a rotatable holder (up to 240 rpm) to obtain homogeneous deposited films at a distance of 0.25 m above the evaporator. The thickness of film samples was measured during deposition using a thickness monitor (Edwards, FTM) and confirmed af-

ter deposition by Tolansky's interferometric method [20]. The chemical composition of the investigated samples was checked by energy dispersive X-ray (EDX) analysis using a JOEL 5400 scanning electron microscope. The structural identification of the investigated compositions in thin film form was confirmed by both X-ray diffraction (XRD) and differential thermal analysis (DTA).

For ac measurements films were sandwiched between two aluminum electrodes of a suitable thickness (500 nm). A programmable automatic RLC bridge (PM 6304Phillips) was used to measure the sample impedance Z, the sample capacitance C_x and loss tangent $\tan\delta$ directly. All investigated samples were represented on the screen of the bridge by a resistance R connected in parallel with capacitance C_x. The total conductivity $\sigma_t(\omega)$ is given by $\sigma_t(\omega) = \frac{1}{z}\frac{L}{a}$, where L is the sample thickness and a is the sample area. The dielectric constant ε_1 was calculated by applying the relation $\varepsilon_1 = \frac{L}{a}\frac{C_x}{\varepsilon_0}$ where ε_0 is the permittivity of free space ($\varepsilon_0 = 8.85 \times 10^{12}$ F/m). The dielectric loss ε_2 was calculated from the relation $\varepsilon_2 = \varepsilon_1 \tan\delta$ where $\delta = 90 - \varphi$, φ is the phase angle. The temperature of the sample was recorded by means of digital multimeter (Protec 81) provided by a chromel–alumel thermocouple adjacent to the sample.

3. Results and discussion

3.1. X-ray diffraction XRD analysis of $Ge_{15}Se_{60}As_{25}$ and $Ge_{15}Se_{60}Sn_{25}$ films

To investigate the structure of the compositions under test in thin film form, films of different thicknesses were thermally deposited under vacuum on glass substrates whose temperature was kept constant at that of the room. X-ray diffraction was carried out for the investigated film compositions. The diffraction patterns obtained for these film compositions are characterized by the absence of any diffraction lines, indicating the amorphous nature of the prepared films. The amorphous nature of the studied samples was confirmed from differential thermal analysis [21].

The investigated compositions in thin films forms were checked using EDX spectroscopy. Analysis indicates that the percentages of the constituent materials in the studied compositions are close to the prepared compositions. Moreover, EDX analysis indicates the absence of impurities elements in the studied compositions.

3.2. Frequency and temperature dependence of ac conductivity

The total conductivity $\sigma_t(\omega)$ is evaluated using the following relation:

$$\sigma_t(\omega) = \frac{1}{z}\frac{L}{a}.$$

The ac conductivity analyzed using the universal feature of ac conductivity in disordered materials given by the following relation [14]:

$$\sigma_{ac}(\omega) = \sigma_t(\omega) - \sigma_{dc} = A\omega^s, \tag{1}$$

where s is the frequency exponent, A is a constant, ω is the circular frequency $\omega = 2\pi f$ and f is the operating frequency, σ_{dc} is the dc conductivity. Ac conductivity $\sigma_{ac}(\omega)$ is calculated by the subtraction of dc conductivity from the total electrical conductivity $\sigma_t(\omega)$. Since the obtained dc conductivity is much smaller than the total conductivity, σ_{dc} can be neglected in Eq. (1), so $\sigma_t(\omega)$ is considered to be $\sigma_{ac}(\omega)$ for the studied film samples.

The variation of $\sigma_{ac}(\omega)$ with frequency was investigated in the range (10^2–10^5 Hz) for films of different thicknesses in the range (89–903 nm) and at different values of temperature in the range (303–413 K) which below the corresponding glass transition temperature [21]. Figure 1 shows the frequency dependence of ac conductivity $\sigma_{ac}(\omega)$ at different temperature for one thickness of each composition as an example. It is clear from the above figure that $\sigma_{ac}(\omega)$ increases linearly with increasing frequency. The same behavior of the frequency dependence of $\sigma_{ac}(\omega)$ was obtained for all the investigated films. Values of the frequency exponent s were calculated from the slopes of the straight lines of Fig. 1. The mean values of the frequency exponent s for samples of different thicknesses for each composition was calculated and plotted as a function of temperature in Fig. 2.

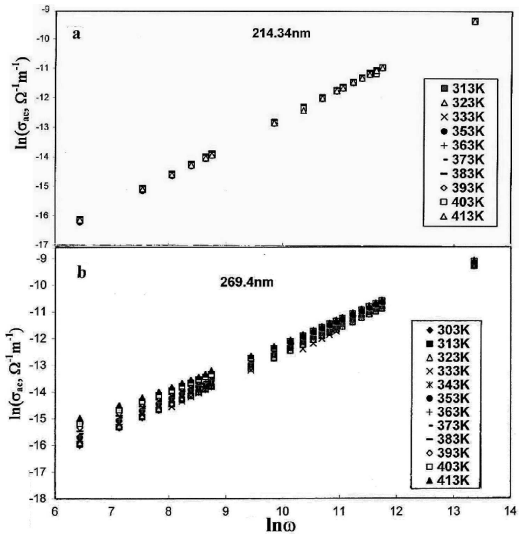

Fig. 1. Frequency dependence of the ac conductivity $\sigma_{ac}(\omega)$ for $Ge_{15}Se_{60}As_{25}$ films (a) and $Ge_{15}Se_{60}Sn_{25}$ films (b) at different temperatures.

It is clear from this figure that the frequency exponent s has values close to unity for $Ge_{15}Se_{60}As_{25}$ and $Ge_{15}Se_{60}Sn_{25}$ films, which decrease slightly with temperature. The same behavior was obtained for all other thicknesses of two compositions.

This behavior is in contradiction with quantum mechanical tunneling (QMT) model [22] which does not predict a temperature dependence of the frequency ex-

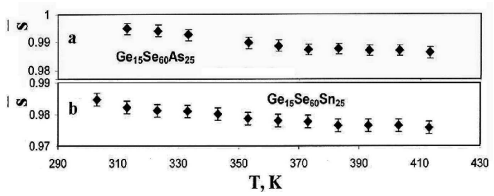

Fig. 2. Temperature dependence of the average value of the frequency exponent s for $Ge_{15}Se_{60}As_{25}$ (a) and $Ge_{15}Se_{60}Sn_{25}$ (b) film samples.

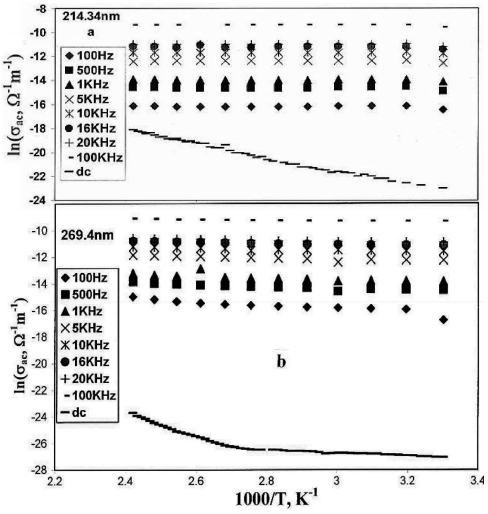

Fig. 3. Temperature dependence of the ac conductivity $\sigma_{ac}(\omega)$ for $Ge_{15}Se_{60}As_{25}$ films (a) and $Ge_{15}Se_{60}Sn_{25}$ films (b) at different frequencies.

ponent s but has a constant value ($s = 0.81$). The correlated barrier hopping (CBH) model [18, 23, 24] predicts a decrease in the value of s for valence alternation pairs (VAP's) centers, while it predicts a very slight decrease in s with temperature values close to unity for intimate VAP's (IVAP's) centers [24–26]. Thus, the obtained data for the temperature dependence of s for the considered films can be explained on the basis of the CBH model between centers forming IVAP's centers.

The variation of $\sigma_{ac}(\omega)$ as a function of temperature at different frequencies for the studied film samples is investigated. Figure 3 shows this variation for one film from each composition as an example. It is clear that the ac conductivity presented in Fig. 3 is temperature activated from different localized states in the gap or its tails and increases linearly for the two compositions (X = As or Sn).

The activation energy $\Delta E(\omega)$ of conduction is calculated at different frequencies using the well-known equation

$$\sigma_{ac}(\omega) = \sigma_0 \exp(-\Delta E(\omega)/k_B T)\,, \qquad (2)$$

where σ_0 is constant.

The values of $\Delta E(\omega)$ are calculated and listed in Table I. It is clear that $\Delta E(\omega)$ decreases with increasing frequency. This decrease may be attributed to the increase of applied field frequency which enhances the electronic jump between the localized states, consequently $\Delta E(\omega)$ decreases as found for other materials [27]. The obtained ac activation energy is much lower than the dc activation energy obtained before [21] over the same range of temperature. The discrepancy between dc and ac activation energies is as expected since the charge carriers in the dc conduction would choose the easiest paths which include the same large jumps, while this is not so important with ac conduction [28]. The smaller values of the ac activation energy and the increase of $\sigma_{ac}(\omega)$ with increasing frequency confirm that the hopping conduction is the dominant mechanism.

TABLE I

Values of the density of states $N(E_f)$ for $Ge_{15}Se_{60}As_{25}$ and $Ge_{15}Se_{60}Sn_{25}$ films at room temperature.

Composition	Frequency [kHz]	$N(E_f)$ [m^{-3}]	$\sigma_{ac}(\omega)$	$\Delta E(\omega)$ [eV]
$Ge_{15}Se_{60}As_{25}$	1	2.055×10^{25}	1.48×10^{-6}	5.00×10^{-4}
	5	2.423×10^{25}	7.0×10^{-6}	3.71×10^{-4}
	10	2.62×10^{25}	1.43×10^{-5}	3×10^{-4}
	20	2.788×10^{25}	2.73×10^{-5}	2.7×10^{-4}
	100	2.83×10^{25}	9.2×10^{-5}	2.5×10^{-4}
$Ge_{15}Se_{60}Sn_{25}$	1	1.678×10^{25}	9.89×10^{-7}	6.16×10^{-5}
	5	1.956×10^{25}	4.69×10^{-6}	5.1×10^{-5}
	10	2.107×10^{25}	9.25×10^{-6}	4.79×10^{-5}
	20	2.283×10^{25}	1.83×10^{-5}	4.23×10^{-5}
	100	2.775×10^{25}	8.82×10^{-5}	3.4×10^{-5}

The analysis of the frequency and temperature dependence of the ac conductivity shows that the obtained data is in agreement with the mechanism proposed by the CBH model. It may be attributed to the correlated barrier hopping mechanism of charge carrier across the defect states D^+ and D^-. Each pair of D^+ and D^- is assumed to form a dipole with a relaxation energy [29–31], which can be attributed to the existence of a potential barrier over which the carriers must hop [32]. It must be noticed here that the process of hopping of charge carriers is affected also by the density of localized states $N(E_f)$, which can be calculated using the following equation [31]:

$$\sigma_{\rm ac}(\omega) = \frac{1}{3}\pi e^2 k_{\rm B} T[N(E_{\rm F})]^2 \alpha^{-5} \omega \left[\ln(\nu_{\rm ph}/\omega)\right]^4 , \quad (3)$$

where e is the electronic charge, $\nu_{\rm ph}$ is the predominant phonon frequency and α the exponential decay parameter of the localized states wave functions. By assuming $\nu_{\rm ph} = 10^{12}$ Hz and $\alpha^{-1} = 10$ Å [33], the density of localized states $N(E_f)$ is calculated at different frequencies and at 303 K for the studied samples. The obtained values of $N(E_f)$ are given in Table I for the studied composition films.

It is observed from this table that there is a significant increase in the density of localized state for As addition rather than Sn addition in the considered compositions. This will lead to increase in the $\sigma_{\rm ac}(\omega)$ at any frequency with As addition (see Table I).

It is known that for amorphous materials the band edges (edges of valence and/or the conduction band) are broadened, mainly by the lack of a long-range order as well as the presence of defects. The addition of As leads to an increase in the density of localized states in the band tail and consequently enhances the ac conductivity.

3.3. Dielectric properties of the studied film compositions

Dielectric analysis measures the electric properties of a material as a function of temperature and frequency. Two fundamental dielectric characteristics of materials are concluded from this analysis: (1) The capacitive (insulating) nature which represents its ability to store electrical charges. (2) The conductive nature which represents its ability to transfer electric charges. Through the dielectric analysis the dielectric constant $\varepsilon_1(\omega)$ and the dielectric loss $\varepsilon_2(\omega)$ for a material can be obtained.

3.3.1. Temperature and frequency dependences of the dielectric constant $\varepsilon_1(\omega)$

The temperature and frequency dependences of the dielectric constant $\varepsilon_1(\omega)$ were studied for the investigated film compositions of different thicknesses in the above mentioned investigated ranges of temperature and frequency.

Figure 4 shows the temperature dependence of dielectric constant ε_1 for one thickness as a representative example for $Ge_{15}Se_{60}As_{25}$ and $Ge_{15}Se_{60}Sn_{25}$ film compositions, respectively. The same behavior was obtained for all other studied films. It is clear from these figures that

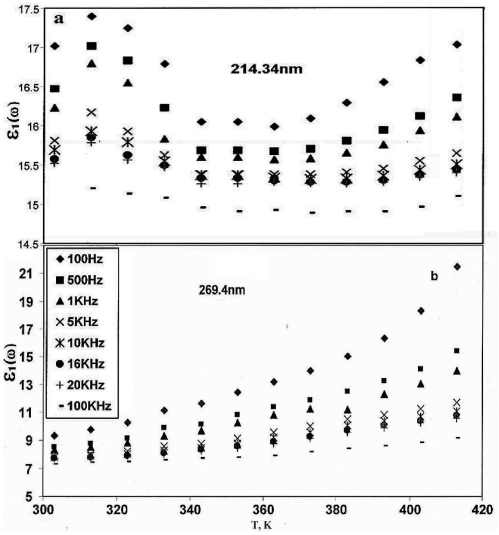

Fig. 4. Temperature dependence of the dielectric constant ε_1 for $Ge_{15}Se_{60}As_{25}$ (a) and $Ge_{15}Se_{60}Sn_{25}$ (b) films at different frequencies.

ε_1 increases as the temperature increases over the whole investigated range of frequency. For the $Ge_{15}Se_{60}As_{25}$ films (Fig. 4a) the common features which characterized the curves is the presence of a maximum. In general, $\varepsilon_1(\omega)$ increases with temperature up to 363 K, which agrees with that obtained for other amorphous semiconductors [34]. Then, $\varepsilon_1(\omega)$ decreases steeply, after which it increases again with temperature. This behavior may be attributed to that of the sample undergoing certain types of transformations which lead to a reordering process of the dipoles.

The increase of ε_1 with temperature can be attributed to the fact that the dipoles in polar materials cannot orient themselves at low temperature. When the temperature is increased the orientation of dipoles is facilitated and thus increases the value of the orientational polarization, which increases ε_1.

Figure 5 show the frequency dependence of the dielectric constant ε_1 at different temperatures for one thickness for each composition as examples. It is clear from this figure that ε_1 decreases with increasing frequency. It is clear from Fig. 5a for $Ge_{15}Se_{60}As_{25}$ films that it was difficult to draw the frequency dependence of $\varepsilon_1(\omega)$ in the temperature range up to 363 K. The variation of ε_1 with frequency is more clear at high values of temperature than at lower values.

The decrease of the dielectric constant with increasing frequency can be interpreted due to the decrease of the different sorts of polarization in the material under study. Different types of polarization (electronic, ionic, orientation and space charge) contribute to the dielectric constant. Firstly, electronic polarization arises from the displacement of valence electrons relative to positive nucleus. This type of polarization occurs at frequencies up to 10^{13}–10^{15} Hz. Ionic polarization represents second

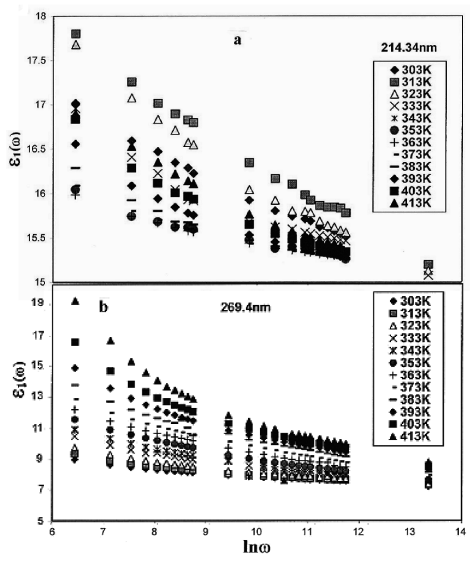

Fig. 5. Frequency dependence of the dielectric constant ε_1 for $Ge_{15}Se_{60}As_{25}$ films (a) and $Ge_{15}Se_{60}Sn_{25}$ films (b) at different temperatures.

type which results from the displacement of ions forming a heteropolar molecule (negative and positive ions with respect to each other). Ionic polarization occurs at frequencies up to 10^{12}–10^{13} Hz. Finally, space charge polarization arises from the impedance mobile charge carrier by interfaces, space charge polarization occurs at frequencies between 1 and 10^3 Hz. The total polarization can be obtained by the sum of these four types of polarization [35]. From this explanation, in the present study the ionic polarization does not play a pronounced effect in the total polarization where the degree of covalent character in the studied samples can be determined with the aid of Pauling relation [36].

The protein of covalent character is equal to

$$100\% \times \exp\left(-0.25(\xi_A - \xi_B)^2\right), \quad (4)$$

where ξ_A and ξ_B are the electronegativity of atoms A and B, respectively. The obtained values of covalent character for the two samples are listed in Table II which explore that in the two studied samples the bonding is predominantly covalent. When the frequency is increased, the orientational polarization decreases since the dipoles will no longer be able to rotate sufficiently rapidly, it takes more time than electronic and ionic polarizations, so that their oscillations begin to lag behind those of the field. As the frequency is raised the permanent dipole, if present in the medium, will be completely unable to follow the field and the orientation polarization ceases, so ε_1 decreases approaching a constant value at a higher frequency due to the interfacial or space charge polarization only.

It is clear from Table III that the values of dielectric constant ε_1 for $Ge_{15}Se_{60}As_{25}$ films are higher than that of $Ge_{15}Se_{60}Sn_{25}$ films. Since the dielectric constant pro-

TABLE II

Calculated covalent character for Ge–Se–X.

Bonds for bond type	% covalent character
Se–Ge	91.39
Se–As	98.79
Se–Sn	95.27
Se–Se	100
As–As	100
As–Ge	96.45
Sn–Sn	100
Sn–Ge	99.36

TABLE III

Values of ε_2 and ε_{2dc} for $Ge_{15}Se_{60}As_{25}$ and $Ge_{15}Se_{60}Sn_{25}$ films at room temperature.

Composition	Frequency	ε_2	ε_{2dc}	ε_1
$Ge_{15}Se_{60}As_{25}$	1 kHz	0.722	1.853×10^{-3}	16.79
	5 kHz	0.646	3.706×10^{-4}	16.16
	10 kHz	0.668	1.85×10^{-4}	15.92
$Ge_{15}Se_{60}Sn_{25}$	1 kHz	1.412	7.538×10^{-5}	8.55
	5 kHz	0.837	1.507×10^{-5}	7.92
	10 kHz	0.86	7.53×10^{-6}	7.81

vides insight into the nature of bonding in the system and from the bond energy values for the studied samples (see Table IV), it is reasonable that the addition of As into Se–Ge increases the weaker bonds in the network structure which are more responsible to the electric field than the stronger bonds with Sn addition. Thus ε_1 for $Ge_{15}Se_{60}As_{25}$ sample is higher than that of $Ge_{15}Se_{60}Sn_{25}$ sample.

3.3.2. The temperature and frequency dependences of the dielectric loss ε_2

The temperature and frequency dependence of dielectric loss ε_2 are investigated for the considered film samples through the ranges of temperature and frequency mentioned above. The obtained variation of ε_2 with temperature at different frequencies is illustrated in Fig. 6 for one thickness as a representative example for each composition. It is clear from this figure that ε_2 increases with increasing temperature. The same behavior was obtained for all studied films.

The obtained relation for the temperature dependence of $\varepsilon_2(\omega)$ for $Ge_{15}Se_{60}As_{25}$ films (Fig. 6a) form a mini-

TABLE IV

Values of bond energy of Se–Sn, Se–As, and Se–Ge.

Bond type	Bond energy [kJ/mol]
Se–Sn	253.35
Se–As	232.36
Se–Ge	254.9

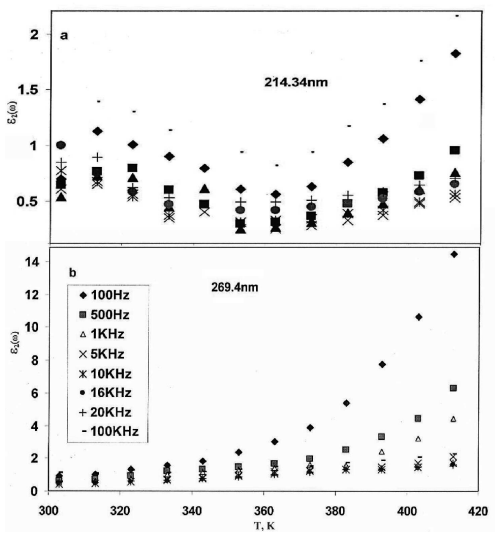

Fig. 6. Temperature dependence of the dielectric loss ε_2 for $Ge_{15}Se_{60}As_{25}$ (a) and $Ge_{15}Se_{60}Sn_{25}$ (b) films at different frequencies.

mum as that for $\varepsilon_1(\omega)$. Such behavior observed in the temperature dependence of $\varepsilon_2(\omega)$ may be attributed to a certain change in the film structure. This change may be resulted in reordering process of the dipoles [34] and consequently disappearing of some components of polarizability in the intermediate range of temperatures at which the anomalous behavior of the temperature dependence of both $\varepsilon_1(\omega)$ and $\varepsilon_2(\omega)$ is observed [34].

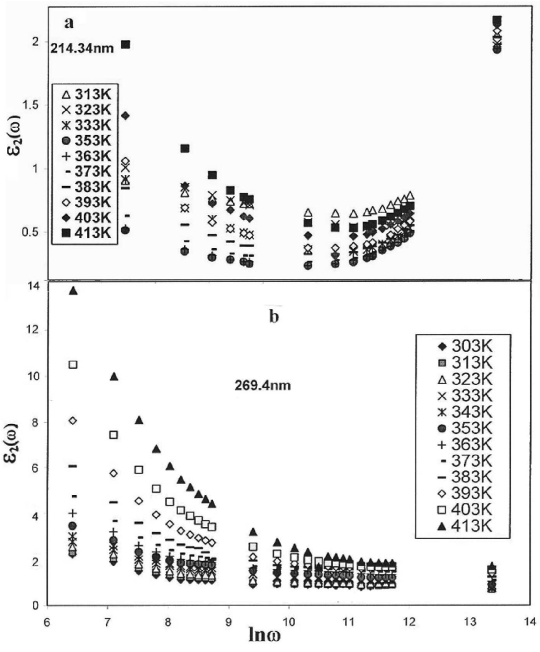

Fig. 7. Frequency dependence of the dielectric loss ε_2 for $Ge_{15}Se_{60}As_{25}$ (a) and $Ge_{15}Se_{60}Sn_{25}$ (b) films at different temperatures.

The dielectric loss consists of two contributions, one from dc conduction and other from the dielectric polarization processes. To study the origin of dielectric loss in the operating temperature range, the dc conduction loss was calculated using the relation $\varepsilon_2 = \sigma_{\rm dc}/\varepsilon_0\omega$, [37] the results are given in Table IV for the studied film samples (for room temperature and frequency = 1 kHz). From this table it is clear that the dc conduction loss is small as compared to ε_2 values obtained from ac measurement, i.e. the dielectric loss cannot be attributed to dc conduction in the entire temperature range. The losses that are attributed to ac conduction presumably involve the migration of ions over large distance. This motion is the same as that occurring under direct current conditions. The ions jump over the highest barriers in the network. As the ions move, they give some of their energy to the lattice as heat and the amount of heat lost per cycle is proportional to $\sigma_{\rm ac}(\omega)/\omega$ [38]. As the temperature increases $\sigma_{\rm ac}(\omega)$ increases and so the ac conduction loss increases with increasing temperature. At low temperature values, conduction, dipole and vibration losses have the minimum value. However at higher temperatures, conduction, dipole and vibration losses all contribute to the dielectric loss.

The frequency dependence of the dielectric loss ε_2 at different temperatures for one thickness as a representative example for each composition is shown in Fig. 7. It is clear from this figure that ε_2 decreases with increasing frequency. But for $Ge_{15}Se_{60}As_{25}$ films (Fig. 7a), the decrease in $\varepsilon_2(\omega)$ with frequency is irregular after 363 K as mentioned above for $\varepsilon_1(\omega)$. This may be attributed also to the change in the film structure.

The decrease of ε_2 with frequency can be attributed to the fact that the migration of ions in the glass is the main source of the dielectric loss at low frequencies. Accordingly, the dielectric loss at low and moderate frequencies is characterized by high values of ε_2 due to the contribution of ion jump and conduction loss of ion migration, in addition to the ion polarization loss. However at high frequencies the ion vibrations may be the only source of dielectric loss.

Mott et al. [39] expressed that when the sample is placed in an electric field, electron hops take place between localized sites. The charge carriers that move between these sites hop from a donor to an acceptor state. In this respect each pair of sites forms a dipole. So, it can be shown that the dielectric properties of chalcogenide glasses can be interpreted, by considering a set of dipoles. As long as the temperature is high enough, which is experimentally verified; below a certain temperature the dielectric permittivity does not depend on temperature. It is supposed that each dipole has a relaxation time depending on its activation energy [29], which can be essentially attributed to the existence of a potential barrier $W_{\rm m}$, over which the carriers must hop [40]. This $W_{\rm m}$, as proposed by Elliott [18, 25], is due to the Coulombic interaction between neighboring sites forming a dipole. We can combine the dielectric loss with the an-

gular frequency (ω) of the applied electric field using the following Eq. [30]:

$$\varepsilon_2(\omega) = (\varepsilon_0 - \varepsilon_\infty)2\pi^2 N(ne^2/\varepsilon_0)^3 k_B T \tau_0^m W_m^{-4} \omega^m \quad (5)$$

with

$$m = -4k_B T/W_m\,, \quad (6)$$

which can be written in the form

$$\varepsilon_2 = B\omega^m, \quad m < 0\,, \quad (7)$$

where ε_∞ is the infinite frequency dielectric constant, and W_m — the energy required to move electron from one site to the infinite.

According to Eq. (7), a plot of $\ln \varepsilon_2(\omega)$ versus $\ln \omega$ yields a straight line whose slope m is negative value. Figure 8 shows $\ln \varepsilon_2(\omega)$ versus $\ln \omega$ at different temperature values through the investigated range for the studied film compositions. It is clear that the obtained relations are straight lines for all films during the corresponding investigated range of temperature. The power m was computed from the negative slopes of the obtained straight lines of the last figures and illustrated as m versus temperature in Fig. 9 for the investigated films. It is obvious that m decreases linearly with increasing temperature for all studied films.

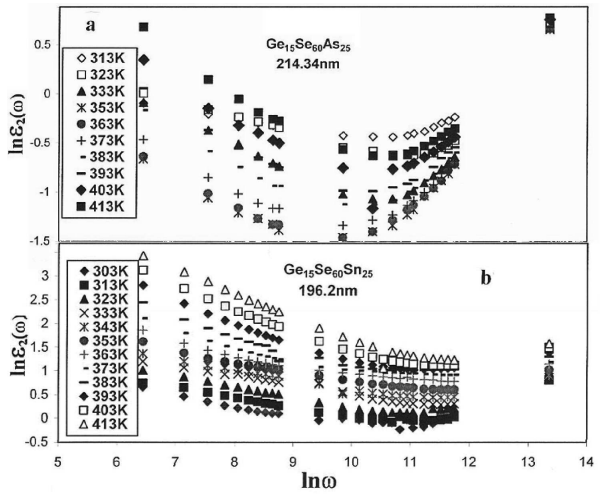

Fig. 8. Plot of $\ln \varepsilon_2$ versus $\ln \omega$ at different temperatures for $Ge_{15}Se_{60}As_{25}$ (a) and $Ge_{15}Se_{60}Sn_{25}$ (b) film samples.

From the slopes of the lines of Fig. 9 for the temperature dependence of m, W_m was calculated according to Eq. (6). The obtained values for W_m are 0.37 and 0.38 eV, respectively, for $Ge_{15}Se_{60}As_{25}$ and $Ge_{15}Se_{60}Sn_{25}$ samples. The obtained values of W_m are in agreement with the theory of hopping of charge carriers over potential barrier as suggested by Elliott [18, 25] in the case of chalcogenide glasses.

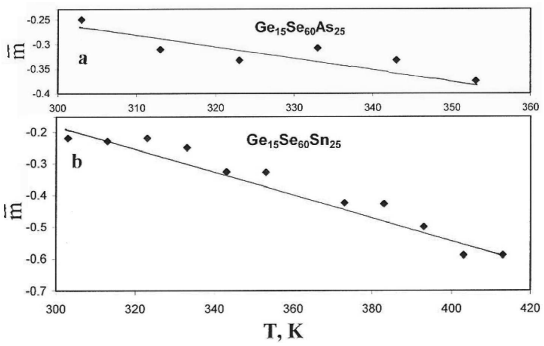

Fig. 9. Temperature dependence of the experimental mean value of m for $Ge_{15}Se_{60}As_{25}$ (a) and $Ge_{15}Se_{60}Sn_{25}$ (b) films.

4. Conclusion

Amorphous thin films of $Ge_{15}Se_{60}X_{25}$ (X = As or Sn) were prepared by thermal evaporation technique. The ac conductivity, dielectric constant and dielectric loss for the studied films were investigated. The results show that the ac conductivity, ε_1 and ε_2 seem likely to be both temperature and frequency dependent. Regarding the frequency dependence of ac conductivity, and the obtained value of s close to unity and slightly decreasing with temperature, the conduction mechanism was suggested to be the hopping between close pairs of centers (IVAP) within the CBH model.

Both frequency and temperature dependence of the dielectric constant ε_1 were attributed to the interfacial and orientational polarization, respectively. Whereas the temperature dependence of dielectric loss ε_2 is associated with the conduction loss. The maximum barrier height was calculated from the dielectric loss for the studied films. The ac parameters were found to be higher for As addition than Sn addition.

References

[1] A.V. Stronski, in: *Proc. NATO Advanced Research Workshop on Micro-electronic Interconnections and Assembly*, Eds. G. Haraman, P. Mach, Kluwer Academic, Netherlands 1998, p. 263.

[2] A. Ganyoo, N. Yoshida, K. Shimakawa, *Recent Res. Dev. Appl. Phys.* **2**, 129 (1999).

[3] M.S. Iovu, S.D. Shutov, M. Popescu, *J. Non-Cryst. Solids*, **299-302**, 924 (2002).

[4] E. Maquez, T. Wagner, J.M. Gonzalez-Leal, A.M. Bemal-Oliva, R. Prieto-Alcon, R. Jimenez--Garay, P.J.S. Ewen, *J. Non.-Cryst. Solids* **274**, 62 (2000).

[5] A. Arsh, M.K. Lebanov, V. Lyubin, L. Shapiro, A. Feigel, M. Veiger, B. Sfez, *Opt.-Mater.* **26**, 301 (2004).

[6] V.F.Lyubin, M. Klebanov, A. Feigel, B. Sfez, *J. Non--Cryst. Solids* **459**, 183 (2004).

[7] R.A. Street, D.K. Biegelsen, *J. Non-Cryst. Solids* **32**, 339 (1979).

[8] P. Agarwal, S. Goel, S.K. Tripathi, A. Kumar, *J. Mater. Sci.* **26**, 4924 (1991).

[9] S. Mahadevan, A. Giridhar, *J. Mater. Sci.* **29**, 3837 (1994).

[10] A.A. Othman, K.A. Aly, A.M. Abousehly, *Thin Solid Films* **515**, 507 (2007).

[11] N.F. Mott, *Philos. Mag.* **34**, 1101 (1976).

[12] S.M. el-Sayed, G.A.M. Amin, *Vacuum* **62**, 353 (2001).

[13] V. Pandly, S.K. Tripathi, A. Kumar, *Physica B* **388**, 200 (2007).

[14] A.K. Sharma, K.L. Bhatia, *J. Non-Cryst. Solids* **109**, 95 (1989).

[15] A. Ghosh, *Phys. Rev. B* **42**, 5665 (1990).

[16] A.C. Warren, J.C. Male, *Electron. Lett.* **6**, 567 (1970).

[17] B. Tareev, *Physics of Dielectric Materials*, Mir, Moscow 1975, p. 42.

[18] S.R. Elliott, *Philos. Mag.* **36**, 1291 (1977).

[19] M.F. Kotkata, H.T. el-Shair, M.A. Afifi, M.M. Abdel Aziz, *J. Appl. Phys.* **27**, 623 (1994).

[20] R.M. Mehra, R. Shyam, P.C. Mathur, *J. Non-Cryst. Solids* **31**, 435 (1979).

[21] M.A. Afifi, N.A. Hegab, H.E. Atyia, M.I. Ismael, *Vacuum* **83**, 326 (2009).

[22] X.H. Leclerc, *J. Phys. (France)* **40**, 27 (1979).

[23] M. Kastener, H. Fritzsche, *Philos. Mag. B* **37**, 199 (1978).

[24] M. Kastener, in: *Proc. 7th Int. Conf. of Amorphous and Liquid Semiconductors*, Ed. W.E. Spear, Edinburgh University 1977, p. 504.

[25] S.R. Elliott, *Solid State Commun.* **27**, 749 (1978).

[26] C. Angell, *Ann. Rev. Phys. Chem.* **43**, 693 (1992).

[27] A.E. Bekheet, N.A. Hegab, *Vacuum* **83**, 391 (2009).

[28] M.A.M. Seyam, A.E. Bekheet, A. Elfalaky, *Eur. Phys.* **16**, 99 (2001).

[29] A.E. Streen, H. Eyring, *J. Chem. Phys.* **5**, 113 (1937).

[30] J.C. Giuntini, J.V. Zanchetta, D. Jullien, R. Enolie, P. Houenou, *J. Non-Cryst. Solids* **45**, 57 (1981).

[31] S.C. Agarwal, S. Guha, K.L. Narasimhan, *J. Non--Cryst. Solids* **18**, 429 (1975).

[32] M. Pollak, G.E. Pike, *Phys. Rev. Lett.* **25**, 1449 (1972).

[33] S. Asokan, M.V.M. Prassad, G. Parathasarathy, E.S.R. Gopal, *Phys. Rev. Lett.* **62**, 808 (1989).

[34] S. Abuo el-Hassan, M. Hammad, *Phys. Status Solidi A* **185**, **2**, 413 (2001).

[35] M. Barsoum, *Fundamentals of Ceramics*, Mc Graw--Hill, New York 1977, p. 543.

[36] L. Pauling, *The Nature of Chemical Bond*, Cornell University, New York 1960.

[37] Nadeem Musahwar, M.A. Majeed Khan, M. Husain, M. Zulfequar, *Physica B* **396**, 81 (2007).

[38] J.M. Stevels, *Handbuch der Physik*, Ed. Flugge, Springer, Berlin 1957, p. 350.

[39] N.F. Mott, E.A. Davis, R.A. Streel, *Philos. Mag.* **32**, 961 (1975).

[40] M. Pollak, G.E. Pike, *Phys. Rev. Lett.* **28**, 1494 (1972).